



# Mechanisms of silver nanoparticle toxicity on the marine cyanobacterium *Prochlorococcus* under environmentally-relevant conditions

Craig J. Dedman<sup>a,\*</sup>, Gabrielle C. Newson<sup>b</sup>, Gemma-Louise Davies<sup>c,\*</sup>, Joseph A. Christie-Oleza<sup>a,d,e,\*\*</sup>

<sup>a</sup> School of Life Sciences, Gibbet Hill Campus, University of Warwick, Coventry CV4 7AL, United Kingdom.

<sup>b</sup> Department of Chemistry, University of Warwick, Gibbet Hill, Coventry CV4 7EQ, United Kingdom.

<sup>c</sup> University College London, Department of Chemistry, 20 Gordon Street, London WC1H 0AJ, United Kingdom.

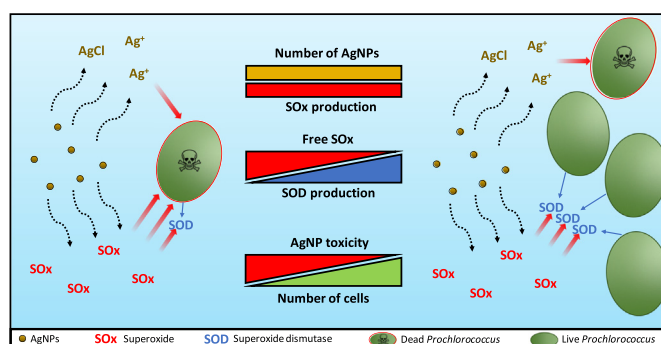
<sup>d</sup> Department of Biology, University of the Balearic Islands, Ctra. Valldemossa, km 7.5, CP: 07122 Palma, Spain

<sup>e</sup> IMEDEA (CSIC-UIB), CP: 07190 Esporles, Spain

## HIGHLIGHTS

- Amongst phytoplankton, *Prochlorococcus* displays highest sensitivity to AgNPs.
- Superoxide as well as leached ionic silver appears to drive AgNP toxicity.
- Environmentally-relevant conditions show close to negligible toxicity on *Prochlorococcus*.
- Particle-to-cell ratio represents a key tool during nanoparticle ecotoxicity assessment.

## GRAPHICAL ABSTRACT



## ARTICLE INFO

### Article history:

Received 21 April 2020

Received in revised form 22 July 2020

Accepted 23 July 2020

Available online 25 July 2020

Editor: Damia Barcelo

### Keywords:

Nanomaterial  
Marine pollution  
Ecotoxicity  
Oxidative stress  
Marine phytoplankton  
*Prochlorococcus*

## ABSTRACT

Global demand for silver nanoparticles (AgNPs), and their inevitable release into the environment, is rapidly increasing. AgNPs display antimicrobial properties and have previously been recorded to exert adverse effects upon marine phytoplankton. However, ecotoxicological research is often compromised by the use of non-ecologically relevant conditions, and the mechanisms of AgNP toxicity under environmental conditions remains unclear. To examine the impact of AgNPs on natural marine communities, a natural assemblage was exposed to citrate-stabilised AgNPs. Here, investigation confirmed that the marine dominant cyanobacteria *Prochlorococcus* is particularly sensitive to AgNP exposure. Whilst *Prochlorococcus* represents the most abundant photosynthetic organism on Earth and contributes significantly to global primary productivity, little ecotoxicological research has been carried out on this cyanobacterium. To address this, *Prochlorococcus* was exposed to citrate-stabilised AgNPs, as well as silver in its ionic form ( $\text{Ag}_2\text{SO}_4$ ), under simulated natural conditions. Both AgNPs and ionic silver were observed to reduce *Prochlorococcus* populations by over 90% at concentrations  $\geq 10 \mu\text{g L}^{-1}$ , representing the upper limit of AgNP concentrations predicted in the environment ( $10 \mu\text{g L}^{-1}$ ). Longer-term assessment revealed this to be a perturbation which was irreversible. Through use of quenching agents for superoxide and hydrogen peroxide, alongside incubations with ionic silver, it was revealed that AgNP toxicity likely arises from synergistic effects of toxic superoxide species generation and leaching of ionic silver. The extent of toxicity was strongly dependent on cell density, and completely mitigated in more cell-dense cultures. Hence, the calculation and reporting of the particle-to-cell ratio reveals that this parameter is effective for standardisation of experimental

\* Corresponding authors.

\*\* Correspondence to: J. Christie-Oleza, Department of Biology, University of the Balearic Islands, Ctra. Valldemossa, km 7.5, CP: 07122, Palma, Spain.

E-mail addresses: [C.Dedman@warwick.ac.uk](mailto:C.Dedman@warwick.ac.uk) (C.J. Dedman), [gemma-louise.davies@ucl.ac.uk](mailto:gemma-louise.davies@ucl.ac.uk) (G.-L. Davies), [joseph.christie@uib.eu](mailto:joseph.christie@uib.eu) (J.A. Christie-Oleza).

work, and allows for direct comparison between studies where cell density may vary. Given the key role that marine cyanobacteria play in global primary production and biogeochemical cycling, their higher susceptibility to AgNP exposure is a concern in hotspots of pollution.

© 2020 The Authors. Published by Elsevier B.V. This is an open access article under the CC BY license (<http://creativecommons.org/licenses/by/4.0/>).

## 1. Introduction

The fate and effects of engineered nanomaterials within the aquatic environment has become a subject of concern and focus of research in recent years (Kalantzi et al., 2019; Stauber et al., 2018; Williams et al., 2019; Zhu et al., 2019). Silver nanoparticles (AgNPs) are present in approximately one quarter of commercially marketed nano-products, primarily because of their antibacterial properties (Sintubin et al., 2012; Vance et al., 2015). This represents the fastest growing class of engineered nanomaterials used for commercial purposes (Fabrega et al., 2011). Global production of AgNPs is currently over 800 metric tonnes *per annum* (Furberg et al., 2016) and is predicted to rise (Syafuddin et al., 2017). The surfaces of AgNPs can be altered to control the release of ionic  $\text{Ag}^+$ , thought to be primarily responsible for their antibacterial properties (Liu et al., 2010). Citrate-stabilised AgNPs represent the most widely used silver colloids for research and commercial purposes (Damm and Munstedt, 2008; Pillai and Kamat, 2003; Tolaymat et al., 2010; Zhang et al., 2011). The widespread use of AgNPs and the significant increase in production of consumer goods utilising nanosized Ag, has increased the likelihood of these particles entering the aquatic environment, either through accidental release, leaching of AgNP-treated surfaces or in wastewater discharge (Benn and Westerhoff, 2008; Kaegi et al., 2010). For example, leaching of AgNPs from outdoor paints has been recorded at concentrations up to  $145 \mu\text{g L}^{-1}$  in runoff events, with 30% total loss of AgNPs over the course of one year (Kaegi et al., 2010). Environmental sampling of nanoparticles remains challenging (Whiteley et al., 2013) and uncertainties exist in the concentrations of engineered nanomaterials predicted in the environment (Holden et al., 2014). Therefore, little evidence exists for the exact concentration of AgNPs within aquatic ecosystems (Maurer-Jones et al., 2013). Current values for surface waters vary according to their proximity to polluting sources and, hence, predicted AgNP concentrations range from those in the  $\text{ng L}^{-1}$  range, up to  $10 \mu\text{g L}^{-1}$  (Maurer-Jones et al., 2013). Due to water fluxes, oceans represent the ultimate sink for these materials.

Approximately one-half of global primary production is carried out by marine phototrophic microorganisms (Field et al., 1998; Flombaum et al., 2013) and, hence, the effect of AgNPs on these organisms is of utmost relevance. However, relatively little evidence exists for the effects of AgNPs upon marine microbial species compared to those from freshwater (Butz et al., 2019). Growth inhibition following AgNP exposure has been previously recorded in a number of marine photosynthetic species (e.g. diatoms (Angel et al., 2013; Burchardt et al., 2012; Gambardella et al., 2015; Huang et al., 2016; Pham, 2018; Pham, 2019; Sendra et al., 2017), green microalgae (Gambardella et al., 2015; Hazeem et al., 2019; Oukarroum et al., 2012a; Oukarroum et al., 2012b; Sendra et al., 2018), marine raphidophytes (He et al., 2012), and cyanobacteria (Burchardt et al., 2012)). Here, AgNPs appear to exert adverse effects upon phytoplankton in a species- and material-specific manner (Gambardella et al., 2015; Huang et al., 2016; Sendra et al., 2018). Typically, ecotoxicological endpoints (*i.e.*  $\text{EC}_{50}$  and  $\text{IC}_{50}$ ) are recorded in the AgNP range of  $24.3 \mu\text{g L}^{-1}$  to  $25.77 \text{ mg L}^{-1}$ , dependent on the model species and specific AgNPs used (Angel et al., 2013; Gambardella et al., 2015; Huang et al., 2016; Pham, 2019; Sendra et al., 2017; Sendra et al., 2018). Often toxic effects are attributed to oxidative stress and damage to cell walls or membranes due to the generation of reactive oxygen species (ROS) or release of toxic silver ions (Choi and Hu, 2008; Liu et al., 2010). Disruption to photosynthetic

processes have also been recorded, such as a decrease in chlorophyll- $\alpha$  content (Hazeem et al., 2019; Pham, 2019), and interference of photosystem-II electron transport (Huang et al., 2016; Oukarroum et al., 2012b). However, it appears that in most studies, high cell-dense, rich-nutrient cultures are used for experimentation with a potential loss of environmental significance. As a result, the exact antimicrobial action of AgNPs under environmentally-relevant conditions remains unclear (Jin et al., 2010).

Here, we provide new evidence for the toxicity of citrate-stabilised AgNPs on natural phytoplankton communities and show how the marine cyanobacteria *Prochlorococcus*, numerically the most abundant phototrophic organism on Earth and major contributor of primary production in oligotrophic oceans (Bagby and Chisholm, 2015; Scanlan et al., 2009), experiences the strongest detrimental effect recorded during community exposure to AgNPs. Using the model *Prochlorococcus* strain MED4 grown under environmentally-relevant conditions (*i.e.* at environmentally-relevant cell densities in natural oligotrophic seawater) we show for the first time that the toxicity and ability of populations to recover from short-term stress caused by AgNP exposure is largely dependent on cell density, a feature often overlooked in ecotoxicological studies upon microbial organisms. The calculation of the particles-to-cell ( $\text{NPs cell}^{-1}$ ) ratio at the beginning of exposures ( $T_0$ ) is presented as an effective tool to account for any variations in cell density, and correctly assess AgNP toxicity. Where appropriate, we promote the consideration of this particles-to-cell value in future research within the field of nano-ecotoxicology. Novel insight into the influence of oxidative stress upon AgNP toxicity under natural conditions is provided, showing that superoxide ( $\text{SOx}$ ) generation, as well as leached ionic silver, plays a key role in *Prochlorococcus*' susceptibility to AgNPs.

## 2. Materials and methods

### 2.1. Materials

Research-grade materials were purchased from Sigma Aldrich, for material-specific purities please see specific sections. Glassware used for experimentation was acid-washed and rinsed in ultrapure Milli-Q water prior to their use.

### 2.2. Natural marine community exposure to AgNPs

Surface seawater (SW) containing its full natural microbial community was obtained from Mallorca, Spain ( $39^{\circ}29'37.9''\text{N}$   $2^{\circ}44'23.4''\text{E}$ , 6th January 2017). 10 mL of SW was incubated in 50 mL tissue culture flasks and exposed in triplicate to a mixed population of laboratory-synthesised citrate-stabilised AgNPs ( $22.0 \pm 3.3 \text{ nm}$  (spheres),  $51.2 \pm 14.9 \text{ nm}$  (rods, length)) at 0, 1 and  $500 \mu\text{g L}^{-1}$ . AgNPs were prepared by the reduction of silver nitrate ( $>99\%$  purity, Sigma Aldrich) by trisodium citrate ( $>99\%$  purity, Sigma Aldrich) and sodium borohydride ( $>99\%$  purity, Sigma Aldrich), as previous (Dong et al., 2010) (full synthesis and characterization data can be found in SI.1, Figs. SI.1 and SI.2). Flasks were incubated at ambient seawater temperature ( $18^{\circ}\text{C}$ ) at a light intensity of  $10 \mu\text{mol photons m}^{-2} \text{ s}^{-1}$  and light:dark cycles of 14:10 h. Phytoplankton communities were monitored by flow cytometry (BD Fortessa) at days 1, 5 and 8, using their distinctive autofluorescence and size to gate the different phototrophic populations (see Section SI.3 for details).

### 2.3. Behaviour and dissolution of AgNPs within natural seawater

Natural SW (station L4, Plymouth, 50°15.0'N; 4°13.0'W) for use in AgNP behaviour and dissolution experiments was prepared by autoclave (20 mins, 120 °C), and subsequently filtered through a 0.22 µm Polyethersulfone membrane (Corning®).

#### a) AgNP behaviour

In order to examine behaviour of AgNPs in natural SW, as prepared above, AgNPs (citrate-stabilised spheres, Sigma Aldrich,  $20.4 \pm 3.9$  nm) were added to 20 mL natural SW at a test concentration of  $1 \text{ mg L}^{-1}$  and maintained at room temperature for a period of 72 h under shaking (100 rpm). At defined timepoints (0, 0.5, 2, 4, 24, 48 and 72 h) a 200 µL subsample was collected from the mid-point of flasks and analysed using Dynamic Light Scattering (DLS) using a Malvern Zetasizer Nano. For each sample, data was collected as the average of 3 measurements made up of 11 readings, each lasting 10 s. To assess aggregation of AgNPs, the alteration in z-average size (d.nm) was recorded at each timepoint. An observation of the mean count rate (kcps) provided insight into the extent of AgNP precipitation out of the water column. The test concentration of  $1 \text{ mg L}^{-1}$  was selected based on preliminary investigation, which revealed this to be the lowest detectable AgNP concentration for reliable data acquisition.

#### b) AgNP dissolution

For monitoring of the dissolution of ionic Ag from AgNPs during the timescale of toxicity testing, AgNP suspensions were made up in 100 mL natural SW, as prepared above, in tissue culture flasks to produce concentrations of 0, 10, 50 and  $250 \text{ µg L}^{-1}$  ( $n = 3$ ). Flasks were maintained under the experimental conditions described above whilst being shaken at 100 rpm. At defined timepoints (0, 0.5, 1, 2, 24, 48, 72, 168 and 240 h), a 5 mL sub-sample was collected from each flask. To ensure AgNPs were effectively removed, ultrafiltration via centrifugation using a Macrosep Advance Centrifugal Device with 10 K Omega Membrane (Pall Laboratory, approximate pore size 2.9 nm) was carried out, as done previously (Angel et al., 2013). Subsequently, filtered natural SW samples were transferred to a new 15 mL falcon tube and stored at  $-20^\circ\text{C}$ . Prior to analysis, samples, including controls, were thawed at room temperature and acid-digested by nitric acid (70%  $\text{HNO}_3$ , Sigma Aldrich) under heating, to remove particulate material and ensure all AgNPs were converted to their ionic form. To remove excess salt, samples were diluted 100× in ultrapure water obtained from a Millipore Milli-Q machine fitted with a 0.22 µm filter operated at 18.2 MΩ at 298 K. Following this, ionic silver content was measured against an internal metal ion standard ( $100 \text{ mg L}^{-1}$  in 5%  $\text{HNO}_3$ ) by inductively coupled atomic emission spectroscopy (ICP-AES) using a Varian 720-ES ICP-AES.

### 2.4. *Prochlorococcus* culture exposure to AgNPs

Axenic *Prochlorococcus* sp. MED4 was routinely grown using Pro99 media (Moore et al., 2002). Prior to AgNPs exposure, *Prochlorococcus* was preadapted to environmentally-relevant conditions by inoculating cells in natural SW (obtained from station L4, Plymouth, 50°15.0'N; 4°13.0'W; filtered through a 0.22 µm polyethersulfone membrane (Corning®) to eliminate particulate organic carbon and further autoclaved for sterility). *Prochlorococcus* was added at close-to-ambient cell densities (i.e.  $10^4 - 10^5$  cells  $\text{mL}^{-1}$ ) (Mella-Flores et al., 2011) and incubated for 72 h under optimal conditions (i.e.  $23^\circ\text{C}$  at constant  $10 \text{ µmol photons m}^{-2} \text{ s}^{-1}$  light intensity using a Lifelite™ full spectrum bulb, with 100 rpm shaking). After 72 h, 30 mL of preadapted *Prochlorococcus* cultures were transferred to 50 mL tissue culture flasks ( $n = 3$ ) and spiked with AgNPs (citrate-stabilised spheres, Sigma Aldrich,  $20.4 \pm 3.9$  nm) at final concentrations of 0, 5, 10, 25 and  $50 \text{ µg L}^{-1}$  as determined by preliminary screening tests (see

Section SI.2 and Fig. SI.3). Cultures were incubated under optimal conditions and monitored by flow cytometry after 0, 6, 24, 48 and 72 h. The particles-to-cell ratio (NPs  $\text{cell}^{-1}$ ) at  $T_0$  was calculated by estimating the number of NPs  $\text{mL}^{-1}$  based on the mass and density of nanoparticles (Metzler et al., 2011; Nemati et al., 1994), and dividing this value by the cyanobacterial cell density recorded by flow cytometry (see Section SI.5). Longer incubations (i.e. 10 days) were set up in both natural SW ( $\sim 3 \times 10^4$  *Prochlorococcus* cell  $\text{mL}^{-1}$ ) and nutrient-rich Pro99 medium ( $\sim 1.8 \times 10^6$  *Prochlorococcus* cell  $\text{mL}^{-1}$ ) to evaluate the ability of cultures to recover after initial stress. AgNPs were spiked at final concentrations of 0, 1, 10, 25, 50,  $250 \text{ µg L}^{-1}$  and cultures were monitored over time by flow cytometry (i.e. 0, 24, 48, 72, 96 and 240 h).

### 2.5. *Prochlorococcus* culture expose to dissolved Ag

Cultures of axenic *Prochlorococcus* sp. MED4 were prepared as described above and exposed to  $\text{Ag}_2\text{SO}_4$  (>99% purity, Sigma Aldrich) under identical experimental conditions following 72 h pre-adaptation. Test concentrations of 0, 0.5, 1, 2.5, 5, 10, 25 and  $50 \text{ µg L}^{-1}$  total Ag ( $n = 3$ ) were established and cyanobacterial populations monitored by flow cytometry, as previous at defined timepoints (0, 6, 24, 48 and 72 h).

### 2.6. Role of reactive oxygen species in the toxicity of AgNPs on *Prochlorococcus*

*Prochlorococcus* sp. MED4 was exposed to AgNPs at a concentration of  $50 \text{ µg L}^{-1}$  under environmentally-relevant conditions (i.e.  $\sim 10^4 - 10^5$  cells  $\text{mL}^{-1}$  in natural SW) and supplemented with sodium pyruvate, a quencher of hydrogen peroxide (Zinser, 2018a); added at 0, 40 and 60 mM (>99% purity, Sigma Aldrich) or superoxide dismutase (SOD; a quencher for SOX; added at  $250 \text{ U mL}^{-1}$ , Sigma Aldrich) during two individual experiments. Cultures were incubated under optimal conditions (see above) for 24 h and cell density was monitored by flow cytometry.

### 2.7. Statistical analysis

For all individual exposures cell density was presented as the mean  $\pm$  standard error ( $n = 3$ ). Any statistical variations between control and treated cultures were identified by means of two-way *t*-tests at each timepoint ( $p \leq 0.05$ ).

## 3. Results and discussion

### 3.1. Effect of AgNP exposure on natural marine phytoplankton communities

Previous studies have revealed the ability of AgNPs to alter marine microbial communities, reducing bacterial growth and diversity (Baptista et al., 2015; Doiron et al., 2012). In particular, photosynthetic microorganisms such as cyanobacteria and diatoms display enhanced sensitivity to AgNPs at concentrations as low as  $0.2 - 2 \text{ µg L}^{-1}$  (Tsiola et al., 2017; Tsiola et al., 2018). To examine the effects of AgNP exposure upon marine phototrophs, natural SW was incubated for a period of 8 days with citrate-stabilised AgNPs at 1 and  $500 \text{ µg L}^{-1}$ . These concentrations were selected to represent predicted environmental and supra-environmental concentrations respectively. A clear reduction of the photosynthetic community as a result of AgNP exposure was observed even at the lowest concentration (i.e.  $1 \text{ µg L}^{-1}$ ;  $\sim 50\%$  cell number decline; Fig. 1). This decline was primarily driven by the decrease in abundance of the cyanobacterial community in accordance with previous studies carried out with natural SW (Tsiola et al., 2018). Here, cyanobacterial decline was mainly of *Prochlorococcus*, displaying 67% and 91% decline in cell numbers at the end of the 8 day incubation in presence of 1 and  $500 \text{ µg L}^{-1}$  of AgNPs, respectively (Fig. 1). In contrast, little or no effect was observed in other phototrophic groups (i.e. pico-



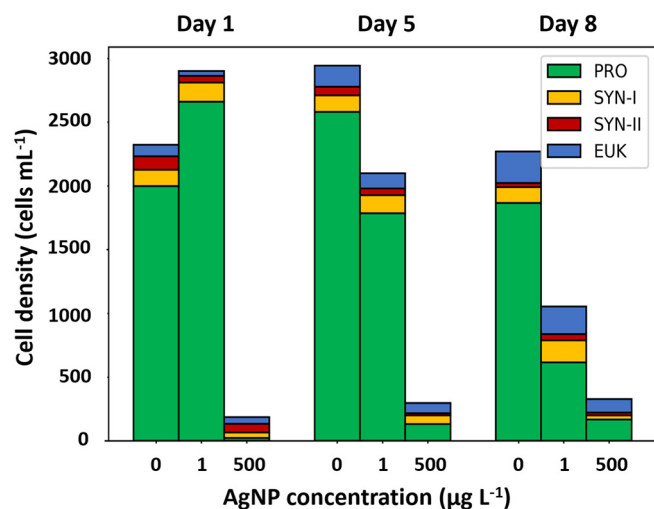


**Fig. 1.** Effect of AgNPs (1 and 500  $\mu\text{g L}^{-1}$ ) upon natural communities of marine phytoplankton. Phytoplanktonic groups are: Green - *Prochlorococcus* (PRO), Yellow - *Synechococcus-I* (SYN-I), Red - *Synechococcus-II* (SYN-II), Blue - *Pico-eukaryotes* (EUK). Data is presented as the mean of three biological replicates ( $n = 3$ ).

eukaryotic or *Synechococcus*) when exposed to the lowest concentration of AgNPs (1  $\mu\text{g L}^{-1}$ ). However, at higher AgNPs concentrations (500  $\mu\text{g L}^{-1}$ ), a cell decline of 57%, 73% and 33% compared to the untreated control was recorded in pico-eukaryotes, and *Synechococcus* subgroups SYN-I and SYN-II, respectively (Fig. 1). AgNPs are believed to exert toxicity primarily via the release of toxic silver ions into media and that other modes of AgNP toxicity are negligible (Xiu et al., 2012). Dissolution of ionic silver from AgNPs within saline media has been reported, and occurs at an increased rate compared to freshwater (Angel et al., 2013; Oukarroum et al., 2012a; Sendra et al., 2017). Silver ions may be released by AgNPs via processes of desorption or oxidation, where the latter produce reactive oxygen species (ROS) as a result (Dobias and Bernier-Latmani, 2013; Liu and Hurt, 2010). Tsiola et al. suggest that the greater sensitivity displayed by marine cyanobacteria is attributed to the increased affinity of AgNPs to sulfur groups present in the cell wall of cyanobacterial cells (Tsiola et al., 2018), thus driving increased interaction between cells and particles by generating silver ions and ROS in close proximity of these organisms. This causing disruption to membrane permeability and deactivation of enzymes, resulting in lysis and cell death (Ratte, 1999). The higher toxicity on *Prochlorococcus* observed here may also be caused by the particularly higher susceptibility of this genus to oxidative stress due to the lack of mechanisms for quenching ROS (Morris et al., 2012).

### 3.2. Behaviour and dissolution of AgNPs in natural seawater

We investigated the behaviour of AgNPs upon entry in natural seawater to help understand how these materials may interact with marine microorganisms and exert their toxic effects. We found that currently available techniques do not provide reliable measurements at the concentrations assayed in this study and discuss these results in the context of higher AgNP concentrations and available literature.

#### a) Aggregation behaviour of AgNPs

The fate and behaviour of nanomaterials within the environment is believed to greatly influence their bioavailability and interaction with biota (Levard et al., 2012; Rodea-Palomares et al., 2010). Dynamic

light scattering (DLS) was utilised to observe the behaviour of AgNPs upon their entry into natural SW. Previously, the aggregation of AgNPs within saline media has been recorded but is often altered by use of nutrient-rich media (Angel et al., 2013; Huang et al., 2016; Oukarroum et al., 2012a; Oukarroum et al., 2012b). As such, natural SW was utilised in this study to maximise environmental relevance. Here, the aggregation of AgNPs was observed to occur immediately upon entry into natural SW (i.e. DLS z-average size of  $122.2 \pm 55.2$  d.nm), increasing to  $271.2 \pm 121.6$  d.nm after 30 min (Table 1 and Suppl. Fig. SI.4A, Section SI.4), as compared to the initial 36.9 d.nm of the AgNP stock prior to addition to SW. This confirms that AgNPs aggregate following their addition to natural SW. Over the subsequent 48 h, z-average size continued to increase, reaching a maximum value of  $964 \pm 104.5$  d.nm. The high variability recorded in z-average size throughout the experiment highlights the large range in AgNP aggregate sizes that are generated once introduced into natural SW. However due to limitations of analytical techniques (Levard et al., 2012), particularly DLS, only concentrations far exceeding those predicted in the environment could be effectively analysed. Studies typically examine AgNP behaviour by utilising concentrations in the range 1–100  $\text{mg L}^{-1}$  (Angel et al., 2013; Huang et al., 2016; Oukarroum et al., 2012a; Oukarroum et al., 2012b). We identified 1  $\text{mg L}^{-1}$  as the minimum concentration that allowed effective data acquisition throughout the 72 h test period which represents 100-fold those predicted in the environment (Maurer-Jones et al., 2013) and that were used in our experiments (see below). Therefore, whilst the potential for AgNPs to aggregate in the marine environment exists, the decreased encounter rate between individual AgNPs caused by dilution in the environment (i.e.  $<10 \mu\text{g L}^{-1}$ ) is likely to cause a considerably reduced aggregation rate under environmentally-relevant concentrations (Furtado et al., 2015; Gottschalk et al., 2013). As such, the true fate and behaviour of AgNPs at environmental concentrations remains uncertain. Interestingly, despite observed AgNP aggregation, examination of the mean count rate revealed that AgNPs and aggregates remained suspended in the water throughout the experiment (see Fig. SI.4B, Section SI.4) with negligible sedimentation of AgNPs as previously recorded (Bertrand et al., 2016). Therefore, AgNPs under environmentally-relevant concentrations will remain bioavailable to planktonic species and other marine biota.

#### b) Dissolution of ionic silver from AgNPs in natural seawater

The release of ionic silver from AgNPs within saline media via dissolution has been widely reported, although only at high concentrations (Angel et al., 2013; Oukarroum et al., 2012a; Sendra et al., 2017). Despite ICP-AES analyses have been utilised for trace metal analyses in seawater in the ppb to ppm range (Berman et al., 1980; Neikov and Yefimov, 2019), the release of ionic silver from AgNPs at the concentration range utilised in this study (i.e. 0–250  $\mu\text{g L}^{-1}$ ) was below the technique's limit of detection. However, previous work examining citrate-stabilised AgNP dissolution (10  $\text{mg L}^{-1}$ ) revealed the process to be slow (Thio

**Table 1**

Z-average size (d.nm) of AgNPs (1  $\text{mg L}^{-1}$ ) suspended in natural seawater for a period of 72 h as measured by Dynamic Light Scattering (DLS).

Time (h)	z-average size (d.nm)
0	122.18 $\pm$ 55.15
0.5	271.21 $\pm$ 121.56
2	379.59 $\pm$ 159.39
4	532.28 $\pm$ 170.53
24	826.39 $\pm$ 106.49
48	964.00 $\pm$ 104.96
72	818.96 $\pm$ 125.50

et al., 2012). Hence, the slow dissolution rate of ionic silver together with the requirement to dilute seawater samples to remove salts prior to analysis, explain why nanoparticle behaviour is typically carried out at relatively high concentrations, way higher than those found in the environment. Such limitations highlight the uncertainty surrounding the mechanisms of AgNP toxicity under environmental conditions.

The rate of silver ion dissolution was described by Jin et al. (2010) as a 'continuous state of flux', dependent on particle size, surface characterization, as well as chemical and biological characteristics of experimental media (Jin et al., 2010; Kittler et al., 2010). Generally, dissolution of AgNPs has been recorded to be higher in saline water versus freshwater by 20-fold (Angel et al., 2013; Graf et al., 2018; Oukarroum et al., 2012a; Sendra et al., 2017). The increased rate of dissolution in marine water has been attributed to the higher concentration of NaCl providing chloride to catalyze the release of silver ions from the particle surface (Sendra et al., 2017). However, despite this increase in dissolution, the specific Ag species formed vary in abundance within freshwater and seawater (Sendra et al., 2017). Sendra et al. (2017) recorded that in freshwater, release of free  $\text{Ag}^+$  can be up to four orders of magnitude above marine. In contrast, colloidal AgCl species dominate ionic silver release into seawater, making up to 99% of dissolved silver content (Angel et al., 2013; Liu and Hurt, 2010; Sendra et al., 2017). Therefore, the larger amounts of free  $\text{Ag}^+$  in freshwater in comparison to marine water is thought to account for the increased toxicity of AgNPs recorded in freshwater, leading researchers to conclude that AgNP release into seawater results in increased dissolution of less toxic Ag species (Angel et al., 2013; Sendra et al., 2017). The behaviour and transformation of AgNPs within the environment will influence this mechanism greatly and, hence, new methods to accurately examine nanoparticle behaviour under environmental conditions are required (Chekli et al., 2015).

### 3.3. Toxicity of AgNPs on *Prochlorococcus*: particles-to-cell ratio matters

Based on the high susceptibility of *Prochlorococcus* to AgNPs observed in the natural community analysis, the strain *Prochlorococcus* sp. MED4 was selected as a model for further laboratory investigation. Experiments were performed mimicking natural environmental conditions (i.e.  $10^4$ – $10^5$  cells  $\text{mL}^{-1}$  in natural SW) (Flombaum et al., 2013) to reduce misleading results caused by high cell density or particle alteration when exposed to enriched media (Romer et al., 2011). Flow cytometric analysis was utilised to monitor cyanobacterial population density following AgNP exposure. Here, given that dead *Prochlorococcus* cells rapidly lose fluorescence (Christie-Oleza et al., 2017; Roth-Rosenberg et al., 2020), any observed reduction in cell counts by flow cytometry would indicate a loss of the living population. A detrimental effect on *Prochlorococcus* sp. MED4 was recorded at AgNP concentrations  $\geq 10 \mu\text{g L}^{-1}$  (Fig. 2A–B), observing a significant population decrease by up to 96% following 72 h exposure (two-way  $t$ -test,  $p \leq 0.05$ ). Cell decline was rapid and clear after only 24 h of exposure to AgNP. Cultured cyanobacteria appeared more resilient than *Prochlorococcus*' natural populations, which suffered a considerable decline at lower AgNP concentrations (i.e.  $1 \mu\text{g L}^{-1}$ ; Fig. 1). Therefore, whilst AgNPs has the potential to exert an adverse effect upon natural cyanobacterial populations, this is likely to occur only in hotspots of AgNP polluted areas where concentrations of these materials reach toxic levels ( $>1 \mu\text{g L}^{-1}$  AgNPs). However, the decline in the phototrophic community in these areas may result in a reduction in primary productivity, with adverse effects upon the surrounding local ecosystem.

Noteworthy, toxicity appeared to differ with varying cell densities, with negative effects of AgNP exposure mitigated by higher cell numbers (Fig. 2A–C). Indeed, no negative effect of AgNP exposure was observed in the most cell-dense culture even at concentrations of  $50 \mu\text{g L}^{-1}$  (Fig. 2C). The effect of varying cell density upon nanomaterial toxicity is a feature that is yet to be investigated in detail, but is one that is likely to vary between studies and experimental runs. As such,

variations in the response observed by organisms due to differing cell density are likely to affect the generation of key ecotoxicological endpoints. Whilst a concentration gradient is typically utilised to investigate the toxicity of a particular substance (i.e.  $\text{EC}_{50}$ ); in the case of nanomaterials this concentration can be considered as the number of particles per volume or per cell, as previously suggested by Metzler et al. (2011) and Unciti-Broceta et al. (2015). However, the use of this parameter is not enforced, resulting in the impossibility to compare studies that use cultures with different cell densities. To aid our understanding of the relationship between AgNP toxicity and cell density, the estimated number of particles-per-cell (NPs  $\text{cell}^{-1}$ ) added at the start of each experiment (including those performed with higher cell densities in enriched seawater, i.e. Pro99 medium) was plotted against the percentage change in cell density after 72 h exposure (Fig. 2D and Supplementary Table S1.2). Interestingly, a strong decline in population was only observed when  $>1000$  NPs  $\text{cell}^{-1}$  was applied, regardless of media type or initial cell concentration (Fig. 2D). This explains the variability in response observed in Fig. 2A–C. It is proposed here that the build-up of ionic silver and associated release of ROS by AgNPs, described below, can be mitigated by denser cell cultures but may become unbearable at a certain threshold. This is particularly damaging to *Prochlorococcus* which lacks appropriate defence mechanisms. Upon consideration of the ambient cell density of microbes in the marine environment ( $\sim 10^6$  cells  $\text{mL}^{-1}$ ) (Vadrucci et al., 2008) and upper limit of AgNPs predicted ( $10 \mu\text{g L}^{-1}$ ) (Maurer-Jones et al., 2013), we are able to estimate a likely maximum environmental NP-cell ratio of 230 NPs  $\text{cell}^{-1}$ . Whilst this value is well below the 1000 NPs  $\text{cell}^{-1}$  threshold we report for *Prochlorococcus* sp. MED4, it may be toxic for natural populations. Nevertheless, in-line with comments above, the current environmental risk of AgNPs appears low and limited to hotspots of AgNP pollution.

It can be argued that altered nanoparticle behaviour within experimental media is likely to reduce accuracy of the NPs  $\text{cell}^{-1}$  ratio calculation. Above, we have shown that there is a potential for AgNPs to aggregate in natural SW (see Section 3.2), thus lowering the effective particle number in suspension during exposure. However, aggregation of AgNPs has only been recorded at concentrations far exceeding those predicted in the environment. We believe that such aggregation will be considerably reduced at the concentrations utilised in this study and predicted in the environment, due to lowered rate of encounter between nanoparticles. Additionally, given that AgNP aggregates were observed to remain in suspension, it is likely that at the low concentration of AgNPs will remain bioavailable in the water column exerting a detrimental effect on marine plankton, as recorded in this study. However, it must be noted that due to the non-defined nature of natural marine seawater, specific water chemistry, dissolved organic matter (Antonio et al., 2015), and particulate content of seawater will vary and influence differently the fate and behaviour of AgNPs (Velzeboer et al., 2014). Hence, despite we account for this by using natural oligotrophic seawater, the impact of such environmental variables must be assessed in future work.

Whilst the NP  $\text{cell}^{-1}$  ratio is likely to vary throughout experimental exposure due to alterations in AgNP behaviour and microbial cell decline, through its application during experimental design, any alteration in cell density shown to cause variation in organismal response is accounted for. Standardisation and direct comparison between studies and experimental replicates is possible as a result. As such, utilisation of this parameter during experimental design proves an effective tool for nano-ecotoxicological investigation upon microbial species.

### 3.4. Ability of *Prochlorococcus* to overcome AgNP stress in long-term exposures

It is expected that upon entry into the aquatic environment, AgNPs are likely to persist for the medium term (i.e. months), with the rate of dissolution dependent on the size and physicochemical properties of particles

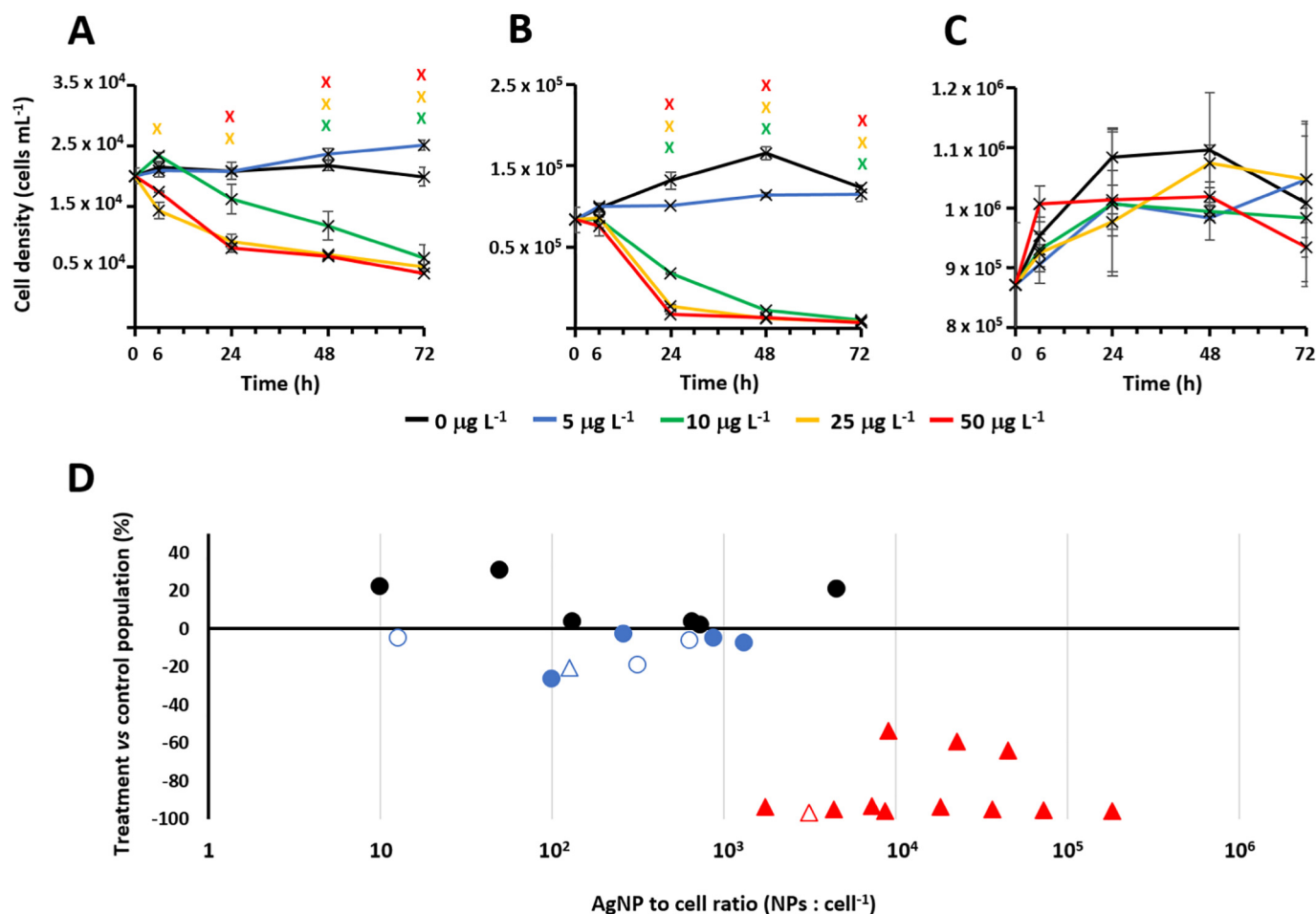


**Fig. 2.** AgNP toxicity on *Prochlorococcus*. Panels A–C display three independent incubation experiments of *Prochlorococcus* grown at varying cell densities when exposed to AgNPs (0, 5, 10, 25, 50  $\mu\text{g L}^{-1}$ ): A –  $2.5 \times 10^4$  cells mL<sup>-1</sup>, B –  $1.3 \times 10^5$  cells mL<sup>-1</sup>, C –  $8.7 \times 10^5$  cells mL<sup>-1</sup>. Data points represent the mean  $\pm$  standard error of three biological replicates ( $n = 3$ ). Significant decreases in cell density due to AgNPs are indicated with crosses (two-way  $t$ -tests;  $p \leq 0.05$ ). Panel D represents the toxic effect of AgNPs on *Prochlorococcus* cultures after 72 h as a function of the nanoparticle-to-cell (NPs cell<sup>-1</sup>) ratio at  $T_0$ . Red markers indicate where cell numbers had decreased >50% versus the control. Triangles indicate cultures with a significant reduction in cells (two-way  $t$ -tests;  $p \leq 0.05$ ). Full and empty markers represent experiments carried out in natural marine seawater and nutrient-rich media (i.e. Pro99), respectively.

(Dobias and Bernier-Latmani, 2013; Kittler et al., 2010). Hence, we assessed if *Prochlorococcus* could overcome the early stress observed within the 72 h exposure over longer incubation periods (i.e. 10 days) in both natural oligotrophic and enriched seawater. As expected, AgNPs ( $\geq 1000$  NPs cell<sup>-1</sup>) produced a strong decrease in the cyanobacterial population in natural SW from which it did not recover (Fig. 3). This response was also observed in higher cell-dense cultures in enriched medium, in which populations did not recover following exposure to concentrations  $>1000$  NPs cell<sup>-1</sup> (see Section SI.6, Fig. SI.5). This demonstrates the inability of *Prochlorococcus* to recover from AgNP-stress and highlights the long-term consequences of such a population decline in areas where AgNP contamination remains high. As a consequence, natural endemic populations are likely to be replaced by other more-resistant species changing community dynamics in polluted areas.

### 3.5. Mechanisms of AgNP toxicity: Superoxide, but not hydrogen peroxide, drives AgNP toxicity on marine cyanobacteria

Despite being an oxygenic photosynthetic organism, *Prochlorococcus* surprisingly lacks mechanisms to effectively quench ROS and is particularly susceptible to oxidative stress (Morris et al., 2012; Regelsberger et al., 2002; Zinser, 2018b). Whilst it lacks catalase to deal with hydrogen peroxide, it does possess a nickel-dependent superoxide dismutase (SOD) essential for the detoxification of SOx (Eitinger, 2004; Scanlan et al., 2009). AgNPs are known to release ROS into the media as a result

of oxidation, and exacerbate cell stress (Liu and Hurt, 2010; Loza et al., 2014). In order to provide insight into the role that ROS plays in the toxicity, *Prochlorococcus* sp. MED4 was incubated with AgNPs in the presence of the H<sub>2</sub>O<sub>2</sub>- or SOx-quenching agents pyruvate (Zinser, 2018a) and SOD, respectively. The test concentration of 50  $\mu\text{g L}^{-1}$  was selected based on evidence of significant cell decline being recorded in previous experimentation. Given that H<sub>2</sub>O<sub>2</sub> is particularly damaging to *Prochlorococcus* (Morris et al., 2011), experiments were first carried out with pyruvate. However, no impact of H<sub>2</sub>O<sub>2</sub>-quenching was recorded, and cell density represented approximately 20–23% of *Prochlorococcus* populations present in control cultures after 24 h. Following this, focus was placed upon SOx. Interestingly, the addition of SOD mitigated the toxicity of AgNPs up to >50% on this relevant marine cyanobacterium (Fig. 4), suggesting that SOx species is a key driver of toxicity in this system. Other ROS such as hydroxyl radical and singlet oxygen may also play a role, but their high reactivity, extremely short half-life in seawater (Zinser, 2018a), and results shown here, suggest these may not be as important. Although, SOx too has a relatively short half-life (Neikov and Yefimov, 2019), the dissolution of AgNPs in the environment is believed to continue for as long as oxygen is available (Liu et al., 2010; Rose, 2012; Zhang et al., 2011) providing a continued SOx production in the local environment through the process of oxidation. SOx is believed to be unable to pass through the cell membrane, therefore SOx produced by AgNP oxidation are likely to interact with the membrane or cell surface (Zinser, 2018a). Previous research

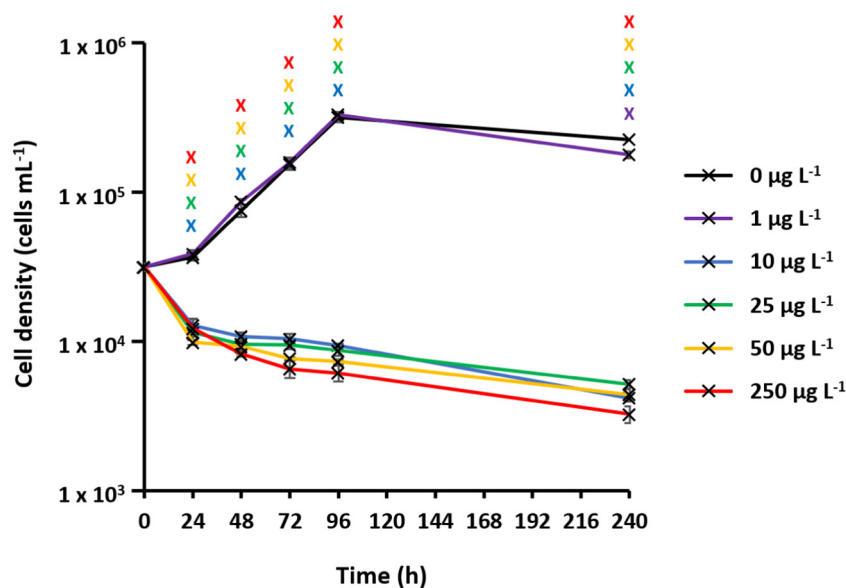


**Fig. 3.** Long-term exposure (10-day) of *Prochlorococcus* to AgNPs (0, 1, 10, 25, 50, 250  $\mu\text{g L}^{-1}$ ) under natural oligotrophic conditions. Data points represent the mean  $\pm$  standard error of three biological replicates ( $n = 3$ ). Significant decreases in cell density recorded in AgNP-treated cultures are indicated by crosses (two-way  $t$ -tests;  $p \leq 0.05$ ).

has also shown that SOx is the most abundant ROS generated intracellularly when bacteria are exposed to AgNPs (Hwang et al., 2008) and, hence, we confirm that this ROS species plays a critical role in driving the antimicrobial action of AgNPs under environmental conditions. This finding also explains the reduced toxicity of AgNPs in cell-dense cultures. The collective production of SOD at a specific cell-to-nanoparticle threshold may counteract the rate at which SOx is produced allowing the culture to overcome ROS toxicity.

### 3.6. Toxicity of dissolved silver on marine cyanobacteria

The antimicrobial action of dissolved silver is widely acknowledged (Xiu et al., 2012). Whilst we were unable to detect ionic silver during ICP analyses under the concentrations tested (Section 3.2b), silver ions are likely to be released by citrate-stabilised AgNPs as recorded when using higher concentrations (1–100  $\mu\text{g L}^{-1}$ ) (Angel et al., 2013).

*Prochlorococcus* cultures were exposed to dissolved silver ( $\text{Ag}_2\text{SO}_4$ ; Fig. S1.6) to determine the toxicity of trace levels of silver leached from AgNPs and that become bioavailable to *Prochlorococcus* during exposure. The impact of dissolved silver upon *Prochlorococcus* was remarkably similar to that recorded in earlier experimentation with AgNPs (Section 3.3; Fig. 2). Following 72 h incubation, *Prochlorococcus* experienced significant cell decline in response to Ag concentrations  $\geq 10 \mu\text{g L}^{-1}$ , resulting in declines of 71.7–95.3% in response to 10–50  $\mu\text{g L}^{-1}$  (two-way  $t$ -test,  $p \leq 0.05$ ; Fig. S1.6). Dissolved silver produced much slower cell declines, requiring 48 h for population depletion as opposed to 24 h needed when exposed to AgNPs. Interestingly, no adverse effect of exposure was recorded at lower concentrations (0.5–5  $\mu\text{g L}^{-1}$ ), indicating little effect of trace Ag levels on this cyanobacterium. Given that similar extents of toxicity are recorded in dissolved silver treatments –where all bioavailable silver is in a dissolved form– and in AgNP treatments –where it is not– it appears that

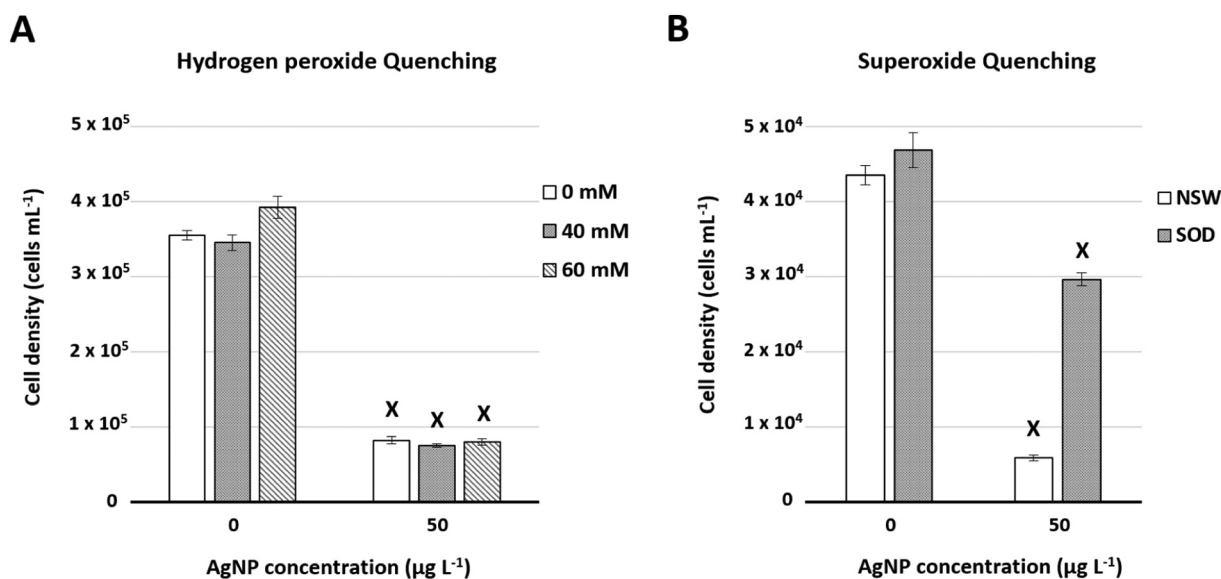


**Fig. 4.** Cell density of *Prochlorococcus* following 24 h growth when exposed to AgNPs (50  $\mu\text{g L}^{-1}$ ) in the presence of A – Pyruvate or B – Superoxide dismutase (SOD) as respective quenchers of hydrogen peroxide and SOx. Data represents the mean  $\pm$  standard error of three biological replicates ( $n = 3$ ). Cultures with a significant decrease in cell number due to AgNP toxicity are indicated with crosses (two-way  $t$ -tests;  $p \leq 0.05$ ). Concentrations of pyruvate used are indicated in panel A. Natural Sea Water (NSW) and SOD (250 U  $\text{mL}^{-1}$ ) is indicated in panel B.



both SO<sub>x</sub> generation and leached silver from nanoparticles drives AgNP toxicity. This result confirms that the remaining decline of *Prochlorococcus* recorded in cultures where SOD was present (Fig. 4) may be attributed to the synergistic adverse effect of any remaining SO<sub>x</sub> species and toxic silver species released from AgNPs. This interaction is likely to occur in close proximity to cyanobacterial cells due to high affinity between AgNPs and the cyanobacterial cell membrane (Tsiola et al., 2018), resulting in localised release of SO<sub>x</sub> and ionic silver through oxidative processes. Here, SO<sub>x</sub> and toxic silver species are likely to disrupt enzymatic processes and induce membrane instability, resulting in cell lysis and death.

#### 4. Conclusions

Under environmentally-relevant conditions citrate-stabilised AgNPs exert a toxic response upon marine phytoplankton, being the dominant cyanobacterium *Prochlorococcus* mostly affected. Given *Prochlorococcus*' contribution to global primary production, any negative effect exerted upon this relevant phytoplanktonic group is likely to affect local ecosystems as a whole due to a decrease in primary productivity or replacement by other more-resistant photosynthetic organisms, disrupting natural marine food chains. However, given current predictions of environmental AgNP concentrations, such adverse effects are likely only to occur at a local level in highly polluted areas. Further investigation into determining accurate field concentrations of AgNPs will aid in effectively evaluating their risk in natural environments. Our findings also revealed that the extent of toxicity was highly dependent on cell density and, hence, future ecotoxicological research with microbial species may need to consider assaying nanoparticles at environmentally-relevant concentrations to achieve useful and informative conclusions. Here, the use of the particle-to-cell ratio (NPs cell<sup>-1</sup>) is presented as an effective parameter to standardize nano-ecotoxicological studies and experimental replicates where cell densities may vary, and is recommended for future work with research-grade nanomaterials. Subsequent investigation into the mechanisms of AgNP toxicity provided an explanation to this particle-to-cell dependency. We showed that ionic silver was not solely responsible for the cell decline recorded in *Prochlorococcus* and, rather, SO<sub>x</sub> is a key driver of AgNP toxicity. Thus, above a particular particle-to-cell ratio (i.e. >1000 AgNPs cell<sup>-1</sup>) the population of *Prochlorococcus* is unable to collectively mitigate the build-up of toxic SO<sub>x</sub> species though the production of SOD, at which point a clear crash in the population is observed. In future, it will be important to consider the impact of AgNPs upon the entire marine microbial community, and assess whether the community-wide response is sufficient to overcome any negative impact of AgNP exposure.

#### CRedit authorship contribution statement

**Craig J. Dedman:** Conceptualization, Data curation, Formal analysis, Funding acquisition, Investigation, Validation, Writing - original draft. **Gabrielle C. Newson:** Investigation, Formal analysis, Writing - review & editing. **Gemma-Louise Davies:** Conceptualization, Formal analysis, Funding acquisition, Supervision, Validation, Visualization, Writing - review & editing. **Joseph A. Christie-Oleza:** Conceptualization, Funding acquisition, Supervision, Validation, Visualization, Writing - original draft.

#### Declaration of competing interest

The authors declare that they have no known competing financial interests or personal relationships that could have appeared to influence the work reported in this paper.

#### Acknowledgements

CJD was supported by the NERC CENTA DTP studentship NE/L002493/1. JAC-O was funded by NERC Independent Research

Fellowship NE/K009044/1, Ramón y Cajal contract RYC-2017-22452 (funded by the Ministry of Science, Innovation and Universities, the National Agency of Research, and the European Social Fund) and MINECO project PID2019-109509RB-I00 (FEDER co-funding). In addition, we thank the BBSRC/EPSC Synthetic Biology Research Centre WISB BB/M017982/1 for access to equipment. We thank Dr. Aguilo-Ferretjans for her help during processing samples, and the technical assistance by Dr. Ramis and the Cellomics Unit (IUNICS, SCT) of the University of the Balearic Islands. We also thank Connor Wells (UCL) for assistance in ICP-AES analysis.

#### Appendix A. Supplementary data

Supplementary data to this article can be found online at <https://doi.org/10.1016/j.scitotenv.2020.141229>.

#### References

- Angel, B.M., Batley, G.E., Jarolimek, C.V., Rogers, N.J., 2013. *Chemosphere* 93, 359–365.
- Antonio, D.C., Cascio, C., Jaksic, Z., Jurasin, D., Lyons, D.M., Nogueira, A.J., Rossi, F., Calzolari, L., 2015. *Mar. Environ. Res.* 111, 162–169.
- Bagby, S.C., Chisholm, S.W., 2015. *ISME J* 9, 2232–2245.
- Baptista, M.S., Miller, R.J., Halewood, E.R., Hanna, S.K., Almeida, C.M., Vasconcelos, V.M., Keller, A.A., Lenihan, H.S., 2015. *Environ. Sci. Technol.* 49, 12968–12974.
- Benn, T.M., Westerhoff, P., 2008. *Environ. Sci. Technol.* 42, 4133–4139.
- Berman, S.S., McLaren, J.W., Willie, S.N., 1980. *Anal. Chem.* 52, 488–492.
- Bertrand, C., Zalouk-Vergnoux, A., Giamberini, L., Poirier, L., Devin, S., Labille, J., Perreine-Ettajani, H., Pagnout, C., Chatel, A., Levard, C., Auffan, M., Mouneyrac, C., 2016. *Environ. Toxicol. Chem.* 35, 2550–2561.
- Burchardt, A.D., Carvalho, R.N., Valente, A., Nativo, P., Gilliland, D., Garcia, C.P., Passarella, R., Pedroni, V., Rossi, F., Lettieri, T., 2012. *Environ. Sci. Technol.* 46, 11336–11344.
- Butz, S.V., Pinckney, J.L., Apte, S.C., Lead, J.R., 2019. *Nanotoxicol.* 15.
- Chekli, L., Zhao, Y.X., Tijing, L.D., Phuntsho, S., Donner, E., Lombi, E., Gao, B.Y., Shon, H.K., 2015. *J. Hazard. Mater.* 284, 190–200.
- Choi, O., Hu, Z., 2008. *Environ. Sci. Technol.* 42, 4583–4588.
- Christie-Oleza, J.A., Sousoni, D., Lloyd, M., Armengaud, J., Scanlan, D.J., 2017. *Nat. Microbiol.* 2, 17100.
- Damm, C., Munstedt, H., 2008. *Appl. Phys. A Mater. Sci. Process.* 91, 479–486.
- Dobias, J., Bernier-Latmani, R., 2013. *Environ. Sci. Technol.* 47, 4140–4146.
- Doiron, K., Pelletier, E., Lemarchand, K., 2012. *Aquat. Toxicol.* 124–125, 22–27.
- Dong, X., Ji, X., Jing, J., Li, M., Li, J., Yang, W., 2010. *J. Phys. Chem.* 114, 2070–2074.
- Eitinger, T., 2004. *J. Bacteriol.* 186, 7821–7825.
- Fabrega, J., Luoma, S.N., Tyler, C.R., Galloway, T.S., Lead, J.R., 2011. *Environ. Int.* 37, 517–531.
- Field, C.B., Behrenfeld, M.J., Randerson, J.T., Falkowski, P., 1998. *Science* 281, 237–240.
- Flombaum, P., Gallegos, J.L., Gordillo, R.A., Rincon, J., Zabala, L.L., Jiao, N., Karl, D.M., Li, W.K., Lomas, M.W., Veneziano, D., Vera, C.S., Vrugt, J.A., Martiny, A.C., 2013. *Proc. Natl. Acad. Sci. U. S. A.* 110, 9824–9829.
- Furberg, A., Arvidsson, R., Molander, S., 2016. *Very Small Flows? Review of the Societal Metabolism of Nanomaterials*. Nova Science Publisher, Inc, Hauppauge, New York.
- Furtado, L.M., Norman, B.C., Xenopoulos, M.A., Frost, P.C., Metcalfe, C.D., Hintelmann, H., 2015. *Environ. Sci. Technol.* 49, 8441–8450.
- Gambardella, C., Costa, E., Piazza, V., Fabbrocini, A., Magi, E., Faimali, M., Garaventa, F., 2015. *Mar. Environ. Res.* 111, 41–49.
- Gottschalk, F., Sun, T., Nowack, B., 2013. *Environ. Pollut.* 181, 287–300.
- Graf, C., Nordmeyer, D., Sengstock, C., Ahlberg, S., Diendorf, J., Raabe, J., Epple, M., Koller, M., Lademann, J., Vogt, A., Rancan, F., Ruhl, E., 2018. *Langmuir* 34, 1506–1519.
- Hazeem, L.J., Kuku, G., Dewailly, E., Slomianny, C., Barras, A., Hamdi, A., Boukherroub, R., Culha, M., Bououdina, M., 2019. *Nanomaterials (Basel)* 9.
- He, D., Dorantes-Aranda, J.J., Waite, T.D., 2012. *Environ. Sci. Technol.* 46, 8731–8738.
- Holden, P.A., Klaessig, F., Turco, R.F., Priester, J.H., Rico, C.M., Avila-Arias, H., Mortimer, M., Pacpaco, K., Gardea-Torresdesy, J.L., 2014. *Environ. Sci. Technol.* 48, 10541–10551.
- Huang, J., Cheng, J., Yi, J., 2016. *J. Appl. Toxicol.* 36, 1343–1354.
- Hwang, E.T., Lee, J.H., Chae, Y.J., Kim, Y.S., Kim, B.C., Sang, B.I., Gu, M.B., 2008. *Small* 4, 746–750.
- Jin, X., Li, M., Wang, J., Maramba-Jones, C., Peng, F., Huang, X., Damoiseaux, R., Hoek, E.M., 2010. *Environ. Sci. Technol.* 44, 7321–7328.
- Kaegi, R., Sinnet, B., Zuleeg, S., Hagendorfer, H., Mueller, E., Vonbank, R., Boller, M., Burkhardt, M., 2010. *Environ. Pollut.* 158, 2900–2905.
- Kalantzi, I., Mylona, K., Toncelli, C., Bucheli, T.D., Knauer, K., Pergantis, S.A., Pitta, P., Tsiola, A., Tsapakis, M., 2019. *J. Nanopart. Res.* 21, 1–26.
- Kittler, S., Greulich, C., Diendorf, J., Koller, M., Epple, M., 2010. *Chem. Mater.* 22, 4548–4554.
- Levard, C., Hotze, E.M., Lowry, G.V., Brown Jr., G.E., 2012. *Environ. Sci. Technol.* 46, 6900–6914.
- Liu, J., Hurt, R.H., 2010. *Environ. Sci. Technol.* 44, 2169–2175.
- Liu, J., Sonshine, D.A., Shervani, S., Hurt, R.H., 2010. *ACS Nano* 4, 6903–6913.
- Loza, K., Diendorf, J., Sengstock, C., Ruiz-Gonzalez, L., Gonzalez-Calbet, J.M., Vallet-Regi, M., Koller, M., Epple, M., 2014. *J. Mater. Chem. B* 2, 1634–1643.
- Maurer-Jones, M.A., Gunsolus, I.L., Murphy, C.J., Haynes, C.L., 2013. *Anal. Chem.* 85, 3036–3049.



- Mella-Flores, D., Mazard, S., Humily, F., Partensky, F., Mahe, F., Bariat, L., Courties, C., Marie, D., Ras, J., Mauriac, R., Jeanthon, C., Mahdi Bendif, E., Ostrowski, M., Scanlan, D.J., Garczarek, L., 2011. *Biogeosciences* 8, 2785–2804.
- Metzler, D.M., Li, M., Erdem, A., Huang, C.P., 2011. *Chem. Eng. J.* 170, 538–546.
- Moore, L.R., Post, A.F., Rocap, G., Chisholm, S.W., 2002. *Limnol. Oceanogr.* 47, 989–996.
- Morris, J.J., Johnson, Z.L., Szul, M.J., Keller, M., Zinser, E.R., 2011. *PLoS One* 6, e16805.
- Morris, J.J., Lenski, R.E., Zinser, E.R., 2012. *MBio* 3.
- Neikov, O.D., Yefimov, N.A., 2019. *Frantsevich Institute for Problems of Materials Science (IPMS), Kiev, Ukraine*. vol. 2 p. 36 ch. 1.
- Nemati, F., Dubernet, C., Colin de Verdiere, A., Poupon, M.F., Treupel-Acar, L., Puisieux, F., Couvreur, P., 1994. *Int. J. Pharm.* 102, 55–62.
- Oukarroum, A., Bras, S., Perreault, F., Popovic, R., 2012a. *Ecotoxicol. Environ. Saf.* 78, 80–85.
- Oukarroum, A., Polchtchikov, S., Perreault, F., Popovic, R., 2012b. *Environ. Sci. Pollut. Res. Int.* 19, 1755–1762.
- Pham, T.-L., 2018. *Turk. J. Fish. Aquat. Sci.* 19, 1009–1016.
- Pham, T.-L., 2019. *Hindawi Journal of Chemistry* 2019, 1–7.
- Pillai, Z.S., Kamat, P.V.J., 2003. *Phys. Chem. B* 108, 945–951.
- Ratte, H.-T., 1999. *Environ. Toxicol. Chem.* 18, 89–108.
- Regelsberger, G., Jakopitsch, C., Plasser, L., Schwaiger, H., Furtmüller, P.G., Peschek, G.A., Zámocký, M., Obinger, C., 2002. *Plant Physiol. Biochem.* 40, 479–490.
- Rodea-Palomares, I., Boltes, K., Fernández-Piñas, F., Leganés, F., García-Calvo, E., Santiago, J., Rosal, R., 2010. *Toxicol. Sci.* 119, 135–145.
- Romer, I., White, T.A., Baalousha, M., Chipman, K., Viant, M.R., Lead, J.R., 2011. *J. Chromatogr. A* 1218, 4226–4233.
- Rose, A.L., 2012. *Front. Microbiol.* 3, 124.
- D. Roth-Rosenberg, D. Aharonovich, T. Luzzatto-Knaan, A. Vogts, L. Zoccarato, F. Eigemann, N. Nago, H.-P. Grossart, M. Voss and D. Sher, *bioRxiv*, 2020, DOI: <https://doi.org/10.1101/657627>.
- Scanlan, D.J., Ostrowski, M., Mazard, S., Dufresne, A., Garczarek, L., Hess, W.R., Post, A.F., Hagemann, M., Paulsen, I., Partensky, F., 2009. *Microbiol. Mol. Biol. Rev.* 73, 249–299.
- Sendra, M., Yeste, M.P., Gatica, J.M., Moreno-Garrido, I., Blasco, J., 2017. *Chemosphere* 179, 279–289.
- Sendra, M., Blasco, J., Araujo, C.V.M., 2018. *Ecol. Indic.* 95, 1053–1067.
- Sintubin, L., Verstraete, W., Boon, N., 2012. *Biotechnol. Bioeng.* 109, 2422–2436.
- Stauber, R.H., Siemer, S., Becker, S., Ding, G.B., Strieth, S., Knauer, S.K., 2018. *ACS Nano* 12, 6351–6359.
- Syafiuddin, A., Salmiati, M.R. Salim, Kueh, A.B.H., Hadibarata, T., Nur, H., 2017. *J. Chin. Chem. Soc.* 64, 732–756.
- Thio, B.J., Montes, M.O., Mahmoud, M.A., Lee, D.W., Zhou, D., Keller, A.A., 2012. *Environ. Sci. Technol.* 46, 6985–6991.
- Tolaymat, T.M., El Badawy, A.M., Genaidy, A., Scheckel, K.G., Luxton, T.P., Suidan, M., 2010. *Sci. Total Environ.* 408, 999–1006.
- Tsiola, A., Pitta, P., Callol, A.J., Kagiorgi, M., Kalantzi, I., Mylona, K., Santi, I., Toncelli, C., Pergantis, S., Tsapakis, M., 2017. *Sci. Total Environ.* 601–602, 1838–1848.
- Tsiola, A., Toncelli, C., Fodelianakis, S., Michoud, G., Bucheli, T.D., Gavrilidou, A., Kagiorgi, M., Kalantzi, I., Knauer, K., Kotoulas, G., Mylona, K., Papadopoulou, E., Psarra, S., Santi, I., Tsapakis, M., Daffonchio, D., Pergantis, S.A., Pittab, P., 2018. *Environ. Sci.: Nano* <https://doi.org/10.1039/c8en00195b>.
- Unciti-Broceta, J.D., Cano-Cortes, V., Altea-Manzano, P., Pernagallo, S., Diaz-Mochon, J.J., Sanchez-Martin, R.M., 2015. *Sci. Rep.* 5, 10091.
- Vadrucci, M.R., Sabetta, L., Fiocca, A., Mazziotti, C., Silvestri, C., Cabrini, M., Guardiani, B., Konjka, E., Evangelopoulos, A., Koutsoubas, D., Basset, A., 2008. *Aquat. Conserv. Mar. Freshwat. Ecosyst.* 18, S88–S104.
- Vance, M.E., Kuiken, T., Vejerano, E.P., McGinnis, S.P., Hochella Jr., M.F., Rejeski, D., Hull, M.S., 2015. *Beilstein J. Nanotechnol.* 6, 1769–1780.
- Velzeboer, I., Quik, J.T., van de Meent, D., Koelmans, A.A., 2014. *Environ. Toxicol. Chem.* 33, 1766–1773.
- Whiteley, C.M., Dalla Valle, M., Jones, K.C., Sweetman, A.J., 2013. *Environ Sci Process Impacts* 15, 2050–2058.
- Williams, R.J., Harrison, S., Keller, V., Kuensen, J., Lofts, S., Praetorius, A., Svendsen, C., Vermeulen, L.C., van Wijnen, J., 2019. *Curr. Opin. Environ. Sustain.* 36, 105–115.
- Xiu, Z.M., Zhang, Q.B., Puppala, H.L., Colvin, V.L., Alvarez, P.J., 2012. *Nano Lett.* 12, 4271–4275.
- Zhang, W., Yao, Y., Sullivan, N., Chen, Y., 2011. *Environ. Sci. Technol.* 45, 4422–4428.
- Zhu, Y., Liu, X., Hu, Y., Wang, R., Chen, M., Wu, J., Wang, Y., Kang, S., Sun, Y., Zhu, M., 2019. *Environ. Res.* 174, 54–60.
- Zinser, E.R., 2018a. *Environ. Microbiol. Rep.* 10, 412–427.
- Zinser, E.R., 2018b. *Environ. Microbiol. Rep.* 10, 399–411.